Supporting Information

Stealth-Like Polysarcosine-Modified Nanoparticles with Low Dye Dose and Long Blood Circulation for Efficient Breast Cancer Pulmonary Metastasis Imaging

Shangyu Chen[1], Peng Zhou[2], Wan Yang[1], Danni Hu[1], Pengfei Chen[1], Pengfei Sun[1], Jun Ling[2*] and Quli Fan[1*]*

a State Key Laboratory of Organic Electronics and Information Displays & Institute of Advanced Materials (IAM), Jiangsu Key Laboratory for Biosensors, Nanjing University of Posts & Telecommunications, Nanjing 210023, China.
b. MOE Key Laboratory of Macromolecular Synthesis and Functionalization, Department of Polymer Science and Engineering, Zhejiang University, Hangzhou, 310027, China.

1. Experiments.

1.1 Materials.

TQF-NH_2 was produced according to our previous reported protocols[1]. Sarcosine *N*-thiocarbox-yanhydride (Sar-NTA) was synthesized according to reported method[2]. 1,2-distearoyl-*sn*-glycero-3-phosphoethanolamine-*N*-[methoxy(polyethylene glycol)-2000] (DSPE-$mPEG_{2k}$) was obtained from Sigma-Aldrich Chemical Co. (Shanghai, China). Dulbecco's modified eagle medium (DMEM), 3-(4,5-dimethylthiazol-2-yl)-2,5-diphenyl tetrazolium bromide (MTT), and macrophage (J774A.1) cells were purchased from KeyGEN BioTECH. Co., Ltd (Nanjing, China).

1.2 Characterization.

TQF-PSar was characterized using nuclear magnetic resonance (NMR) spectroscopy with a Bruker Ultra Shield Plus 400 MHz (^{1}H) spectrometer. Tetramethylsilane (TMS) was selected as the internal standard and used at 298 K with DMSO-d_6 as the solvent for measurement. Gel permeation chromatography (GPC) was conducted on hexafluoroisopropanol (HFIP) series columns (HFIP-803 and HFIP-805 from Shodex, MW between 1,000 and 600,000). The size and morphology of the prepared nanoparticles were characterized by transmission electron microscopy (HT7700, TEM), whose acceleration voltage is 100 KV. Dynamic light scattering (DLS) analysis was characterized by a commercial laser light scattering spectrometer (ALV-7004, Langen, Germany). The average hydrodynamic diameter was extracted according to the scattering intensity through a CONTIN analysis. All samples were optically cleared with 450 nm Millipore filters before test and the test was conducted with a scattering angle of 90° under room temperature. Zeta potentials were used a zeta potential analyzer at room temperature (Brookhaven ZetaPALS). UV-vis-NIR (Shimadzu UV-3600) spectrophotometer and NIR-II spectrophotometer (Fluorolog 3, Horiba) were used to record the absorption and fluorescence spectra of samples. The 3-(4,5-dimethylthiazol-2-yl)-2,5-diphenyltetrazolium bromide (MTT) assay was carried out on A PowerWave XS/XS2 microplate spectrophotometer (BioTek, Winooski, VT). The NIR-II fluorescence imaging (FLI) experiments were performed by the NIR-II imaging system (Wuhan Grand-imaging Technology Co., Ltd) with an 808 nm diode laser (40 mW cm^{-2}). A 640 × 512-pixel two-dimensional InGaAs array from Princeton Instruments in NIR-II fluorescence windows was equipped in this NIR-II FLI system.

1.3 Synthesis of TQF-PSar.

The polymerization was carried out in pre-dried vials at 60 °C under argon atmosphere. As a typical polymerization of Sar-NTA initiated by TQF-NH_2, Sar-NTA (0.0872 g, 6.649 mmol) was dissolved in acetonitrile (ACN, 12.3 mL), followed by 1.0 mL dichloromethane (DCM) solution of TQF-NH_2 (0.06643 mol/L). After polymerization for 41 hours, the product was purified in ether and dried in vacuo (yield: 64.4%).

1.4 Preparation of Water-Soluble TQF-PSar and TQF NPs.

TQF-PSar can be directly soluble in water for subsequent experiments. For TQF-PEG NPs, TQF hydrophobic dye (1 mg mL^{-1}) in tetrahydrofuran (1.5 mL) was quickly added into deionized water (10 mL) containing DSPE-$mPEG_{2k}$ (15 mg) under continuous ultrasonic dispersion for 8 min. Then the tetrahydrofuran was removed by blowing nitrogen gas on the surface of the solution and the water-soluble TQF-PEG NPs were achieved.

1.5 NIR-II fluorescence quantum yield (QY) test.

The NIR-II fluorescence QY of samples was tested using the method described in a previous study[3]. IR 1061 was used as the reference dye (QY = 1.7 ± 0.5% in dichloromethane (DCM)). The fluorescence spectra of five different concentrations around or less than an OD (at 808 nm) of 0.1 (approximately 0.1, 0.08, 0.06, 0.04 and 0.02) was collected with 808 nm laser. After comparing the slopes of the integrated fluorescence (emission at 1000-1500 nm for NIR-II QY), which was plotted against the absorbance for both the reference and samples, the QY were calculated according to the following equation:

$$QY_{(sample)} = QY_{(ref)} \times \frac{slope_{(sample)}}{slope_{(ref)}} \times \frac{n^2_{(sample)}}{n^2_{(ref)}}$$

Where $QY_{(sample)}$ is the QY of the tested sample, $QY_{(ref)}$ is the QY of IR 1061, $Slope_{(sample)}$ and $slope_{(ref)}$ are the slopes obtained by linear fitting of the integrated emission spectra of the tested samples and IR 1061, respectively. The parameter n is the refractive index of solvents (DCM and water).

1.6 Cell Culture, Cytotoxicity, Cell Uptake, and Cell Association Assay.

All cells were cultured with DMEM containing 10% fetal bovine serum (FBS) in a humidified 5% CO_2 environment at 37 °C. The MTT assay was examined to study the cytotoxicity of TQF-PSar to 3T3 and 4T1 cells at different concentrations (range from 0 to 0.1 mg mL^{-1}). Add 20 μL of MTT into each well of 96-well plate for formazan crystals with another 4 h incubation. Following the remove of upper supernatant, these formazan crystals were lysed by the addition of 100 μL of DMSO with 10 min shake for uniform mixing. Finally, use the Bio-tek Synergy HTX microplate spectrophotometer to determine the 450 nm absorbance of each well. In order to study the specific cellular uptake ability of TQF-PSar to macrophages, both macrophage J774A.1 and tumor 4T1 cells were cultured in six-well plates for 24 h, respectively. Then DMEM was removed followed by washing with PBS. After that, 2.5 μg mL^{-1} (concentration of TQF dye) nanoparticles were added to the cells and co-cultured for another 12 h. After washing with PBS twice to remove the excess nanoparticles, the specific cellular uptake ability and cell association of TQF-PSar to cells were determined according to the NIR-II signals with an NIR-II imaging system.

1.7 Animals and Breast Cancer Pulmonary Metastasis Model.

All animal experiments were carried out in accordance with the specifications of The National Regulation of China for Care and Use of Laboratory Animals, which have been approved by the Jiangsu Administration of Experimental Animals. The breast cancer pulmonary metastasis model mice were constructed by the tail vein injection of 50 μL 4T1 cell suspension.

1.8 *In Vivo* NIR-II Fluorescence Imaging.

The *in vivo* NIR-II imaging of mice was obtained with a commercial NIR-II fluorescence imaging system (Wuhan Grand-imaging Technology Co., Ltd), which was filtered with a 1064 nm

LP filter and excited by an 808 nm laser. The mice were anaesthetized with 3% isoflurane. All samples were injected intravenously.

1.9. Calculation method of signal-to-background ratio (SBR).

The imaging SBR was calculated according to the following equation:

$$SBR = \frac{I_s}{I_n}$$

The parameters Is and In represent the fluorescence signal of the interested region and the noise signal of normal tissue far away from the region of interest, respectively.

2 Figures and discussion.

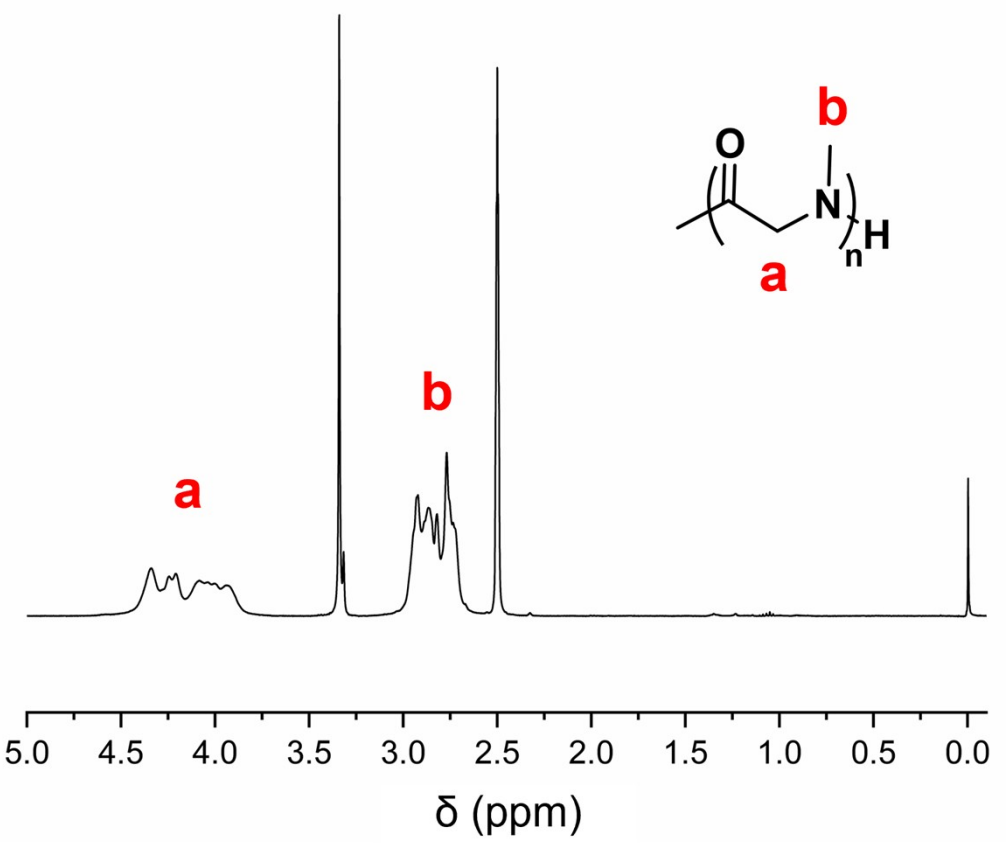

Figure S1. ^{1}H NMR spectrum of TQF-PSar in DMSO-d_6.

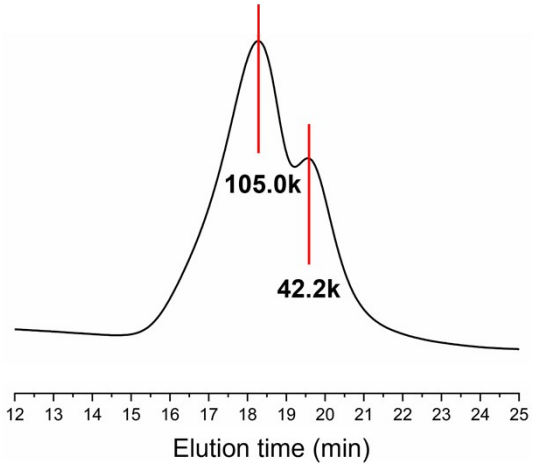

Figure S2. Gel permeation chromatography (GPC) profile of TQF-PSar with HFIP as elution.

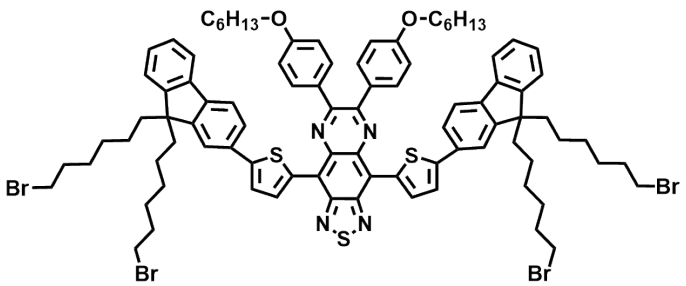

Figure S3. The chemical structure of TQF.

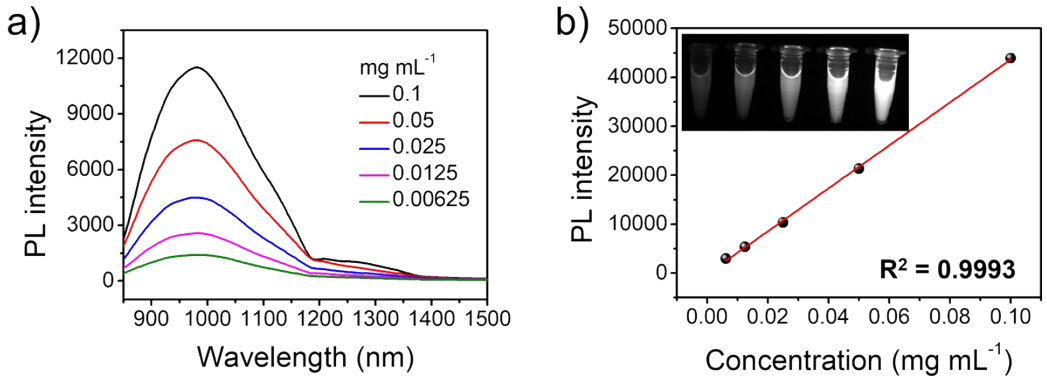

Figure S4. (a) Fluorescence emission spectra of TQF in THF at different concentrations. (b) The corresponding NIR-II images of TQF in tube and their quantified NIR-II fluorescence intensity.

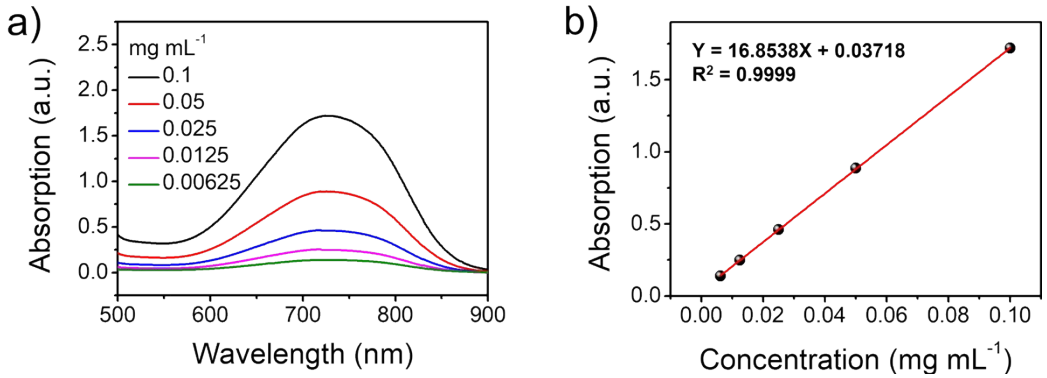

Figure S5. (a) UV-vis-NIR absorption spectra of TQF in THF at different concentrations. (b) Quantified results of TQF absorption intensity at different concentrations.

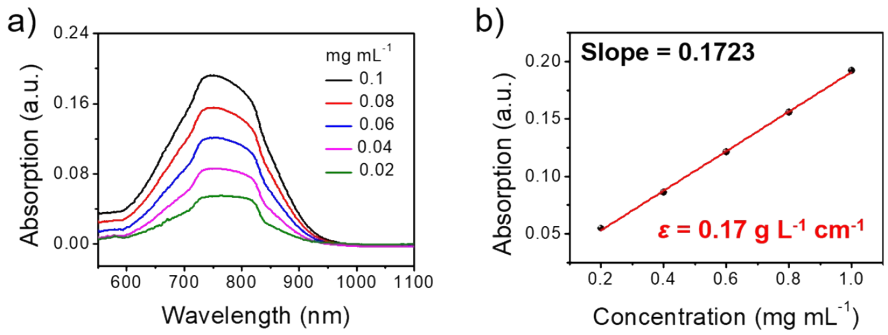

Figure S6. (a) UV-vis-NIR spectra of TQF-PSar in water at different concentration. (b) The mole extinction coefficient of TQF-PSar at 751 nm.

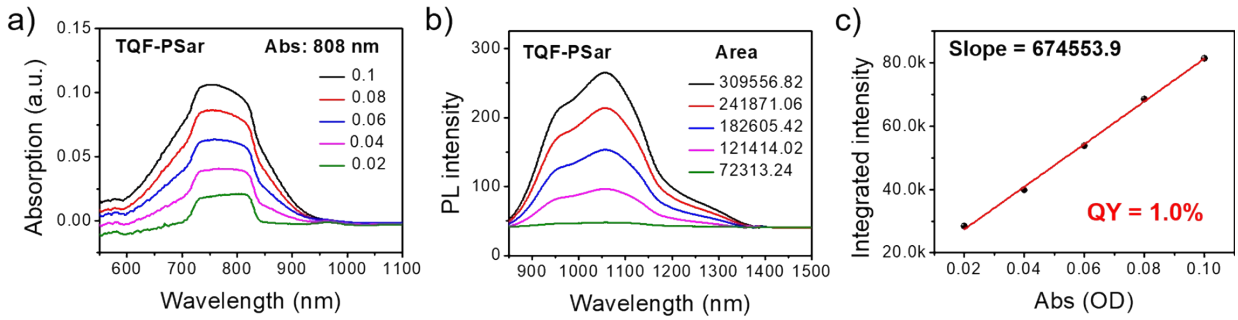

Figure S7. Quantum yield measurement of TQF-PSar. (a) Absorption spectra, (b) fluorescence emission spectra, and (c) relatively quantified analysis of TQF-PSar in water.

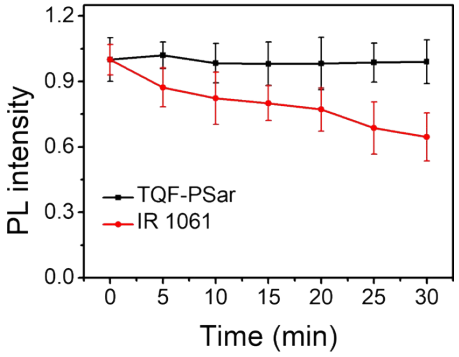

Figure S8. Photo-stability of TQF-PSar and IR 1061 after irradiation of 808 nm laser for 30 min.

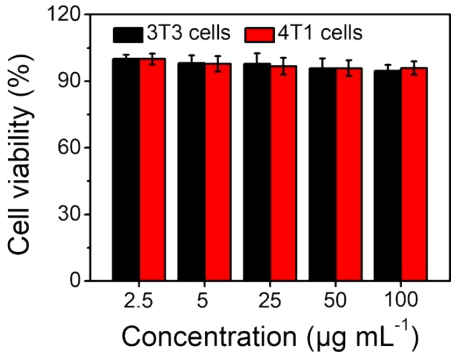

Figure S9. Viability of 3T3 and 4T1 cells after incubation with TQF-PEG NPs at various concentrations (2.5–100 μg mL^{-1}) under darkness for 24 h.

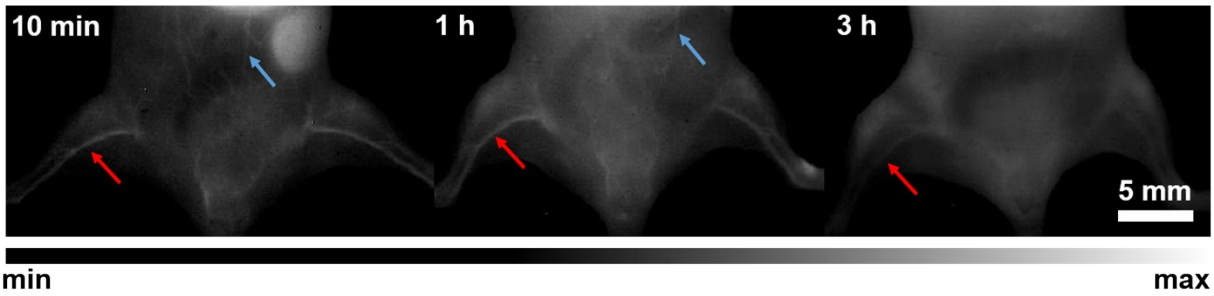

Figure S10. NIR-II FLI of blood vessels in healthy mice (n = 3) at interval times after tail vein injection of TQF-PEG NPs at a dye concentration of 100 μg mL^{-1} (150 μL). Scar bar: 5 mm. Error bars, mean ± s.d. (n = 3).

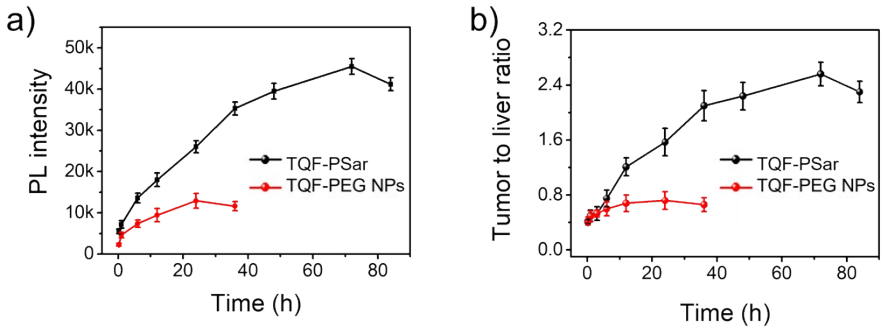

Figure S11. (a) The corresponding NIR-II fluorescence intensity of tumor and (b) quantified ratio of tumor to liver signal in Figure 4a at various times.

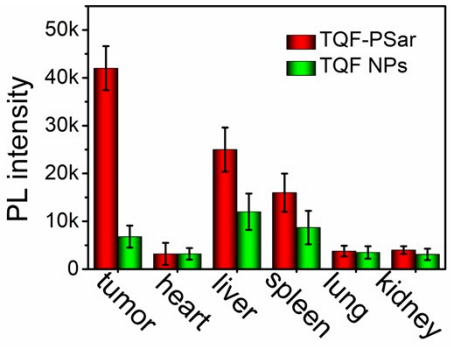

Figure S12. Biodistribution of TQF-PSar and TQF-PEG NPs estimated by their corresponding NIR-II fluorescence intensity in Figure 4e.

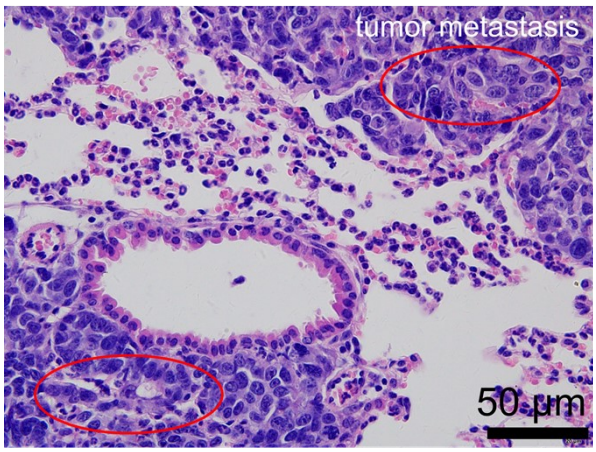

Figure S13. The pathological image of lung from the breast cancer pulmonary metastasis mice.

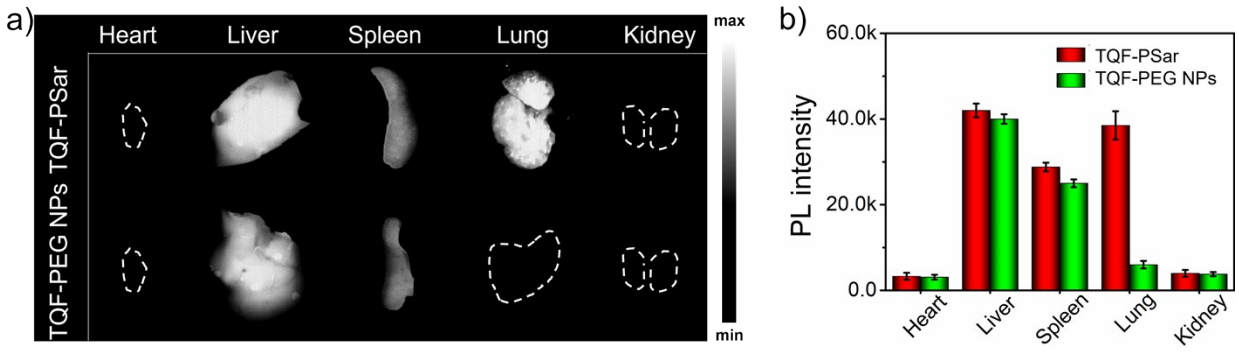

Figure S14. (a) *Ex vivo* NIR-II fluorescence images of the main organs from the different groups and (b) their corresponding quantified NIR-II fluorescence intensity.

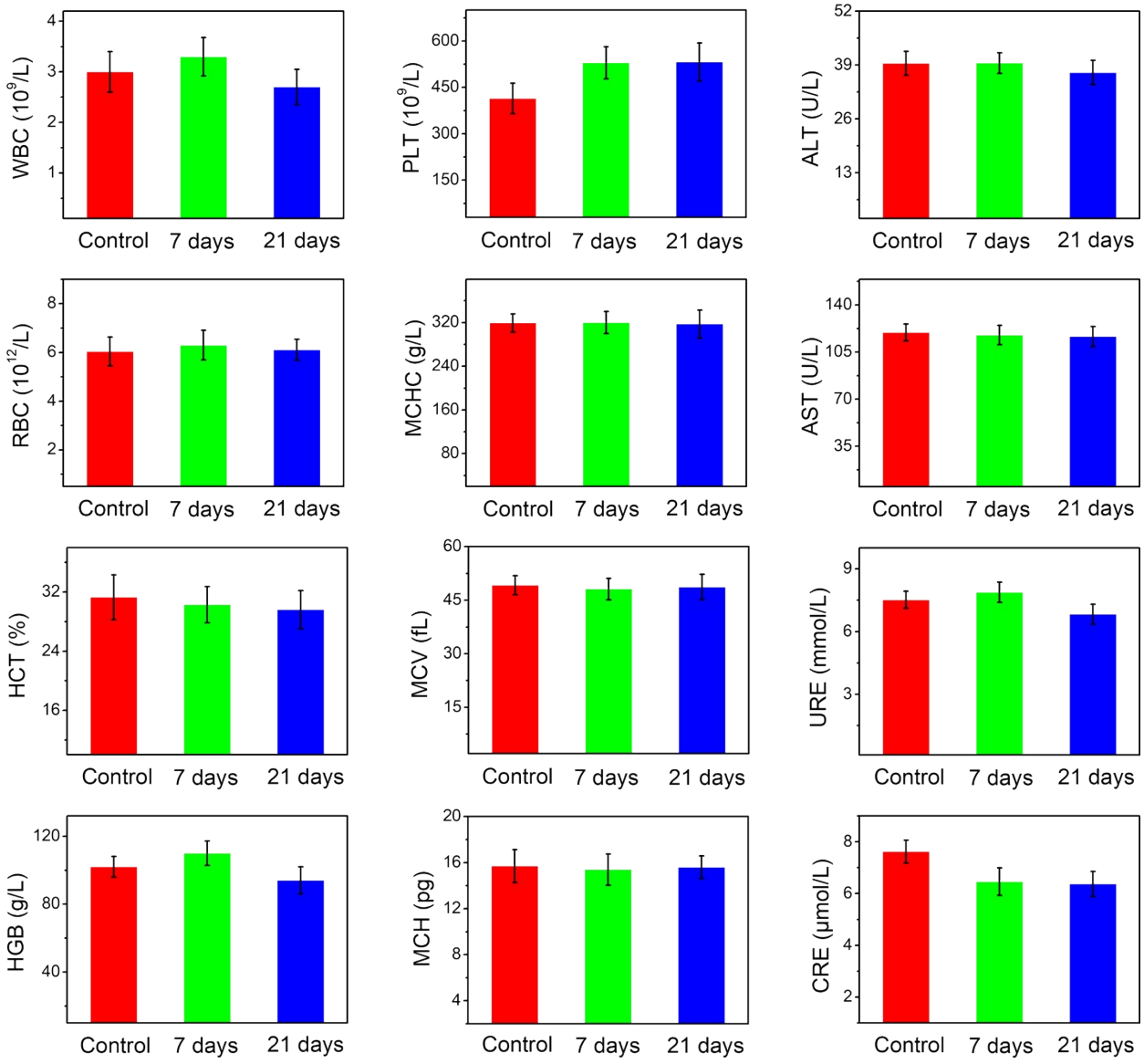

Figure S15. Blood routine tests of mice treated with TQF-PSar. Error bars, mean ± s.d. (n = 3).

3 Reference.

1 Chen S, Miao H, Jiang X, et al. *Biomaterials*, 2021, 275: 120916

2 Tao X, Deng C, Ling J. *Macromol Rapid Commun*, 2014, 35: 875-881

3 Yang Q, Hu Z, Zhu S, et al. *J Am Chem Soc*, 2018, 140: 1715-1724